Determining Quantum Molecular Potentials from Spectroscopic Energy Levels Using Parametric Equations of Motion

David A. Mazziotti[†] and Herschel A. Rabitz[‡]

Department of Chemistry, Harvard University, Cambridge, Massachusetts 02138, and Department of Chemistry, Princeton University, Princeton, New Jersey 08544

Received: May 11, 2000; In Final Form: August 11, 2000

A system of differential equations is presented for evolving the quantum potential as a function of its energy levels. These inverse parametric equations of motion (i-PEM) offer a novel approach to determining quantum molecular potentials from spectroscopic energy levels. The technique uses singular-value decomposition to ensure that the chosen trajectory through energy space is representable by a smooth potential trajectory. The i-PEM are facilitated by discretizing the vibrational Schrödinger equation with a spectral element method which combines the features of Hamiltonian sparsity and exponential convergence of the wave function. Often, spectroscopic data significantly affect only a specific region of the potential, and the spectral elements offer a natural framework for identifying the appropriate portion of the potential. The i-PEM with spectral elements are applied in a simulation for determining the potential of hydrogen fluoride.

I. Introduction

The rotational and vibrational energy level spacings of a molecule contain valuable information about the underlying potential energy surface. The ability to transform spectroscopic energy data into useful potential energy surfaces has been an important source of chemical information, but practical difficulties have often limited the ability to extract quantitative potential information. Since the points on the potential surface are electronic energies, a robust inversion procedure would also furnish a novel approach to supplement electronic structure calculations within the Born−Oppenheimer approximation. Inversion methods analogous to those for potential surfaces apply beyond chemistry to ill-posed problems[1,2] in areas as diverse as medicine[3] and engineering.[4] Within electronic structure, both the density functional theory (DFT)[5] and the *N*-representability problem[6−9] may be characterized as ill-posed problems. Ill-posed problems arise when there is not enough information to define a mathematically precise answer and yet intuitively there seems to be enough information to generate a realistic solution through the inclusion of additional natural constraints such as smoothness. While the Rydberg−Klein−Rees (RKR) technique for calculating potential curves of diatomic molecules has existed for many years,[10] more general techniques that employ the regularization machinery for ill-posed problems have recently been developed to determine the potential energy surfaces for diatomic and other molecules including van der Waals clusters from spectroscopic data.[11−15]

The purpose of this paper is to introduce a new approach for the inversion of spectroscopic energy data. The present method differs in several key respects from existing inversion techniques. Earlier works have introduced a system of differential equations, known as the parametric equations of motion (PEM), for energy eigenvalues and eigenvectors as functions of parameters in the Hamiltonian.[16−19] Here we show how the PEM method may be modified to follow the potential as a function of the energy levels.[17] These inverse parametric equations of motion (i-PEM) allow for the evolution of an initial model potential to a final potential which is fully consistent with the spectroscopically observed energy levels. Most iterative techniques for spectral inversion linearize the relationship between the energy and the potential unknowns by invoking first-order perturbation theory.[11] The i-PEM can naturally use higher orders of perturbation theory to take large steps along a trajectory to identify the potential. Only an initial solution of the Schrödinger equation is required in the iterative inverse procedure, after which the i-PEM formulation implicitly reveals the appropriate solution. Second, the present approach applies the spectral element method,[20−23] which has been used extensively in solving partial differential equations in engineering, for the solution of the rovibrational Schrödinger equation. The advantages of spectral elements include the exponential convergence of spectral methods, matrix sparsity, and weak coupling between different regions of the potential surface. This last feature of spectral elements is especially useful because it allows for altering just a piece of the potential energy surface without modifying the other pieces. Often, the spectroscopic data will only be relevant for improving a specific region of the surface, and the division of the potential into elements is ideal for accomplishing these selective changes. Third, the portion of the potential to be modified is expanded in terms of Legendre polynomials whose coefficients are evolved by the i-PEM as functions of the spectral energies. The exponential convergence of the Legendre polynomials over a finite interval helps to extract the maximum amount of information from the known energies.[22] Finally, the method possesses a strategy for making efficient the evolution from the initial spectral energies to the final target energies. At each point on the trajectory, the i-PEM choose the differential energy changes to make the energies at the next point as close as possible to the target energies while preventing the potential from becoming ill-behaved. To illustrate

[†] Harvard University.
[‡] Princeton University.

10.1021/jp001767g CCC: $19.00
Published on Web 10/07/2000

this technique for inversion, we utilize the i-PEM to simulate the determination of the potential for hydrogen fluoride from a set of Morse vibrational energies.

II. Theory

A. Inverse Parametric Equations of Motion. Consider the Schrödinger equation

$$H(\lambda)\psi_n(\lambda) = E_n(\lambda)\psi_n(\lambda) \tag{1}$$

with the normalization condition

$$\langle\psi_n(\lambda)|\psi_n(\lambda)\rangle = 1 \tag{2}$$

where λ is a parameter in the Hamiltonian. The wave function $\psi_n(\lambda)$ may be expanded in a set of orthonormal basis functions $|\phi_i\rangle$

$$\psi_n(\lambda) = \mathbf{\Phi}\mathbf{C}_n(\lambda) \tag{3}$$

in which $\mathbf{\Phi}$ is the row vector whose elements are the sets $|\phi_i\rangle$ and $\mathbf{C}_n(\lambda)$ is the column vector whose elements are the expansion coefficients $c_{i,n}(\lambda)$. By substituting eq 3 into eqs 1 and 2 and multiplying by $\mathbf{\Phi}^\dagger$, we generate the eigenvalue equation

$$\mathbf{H}(\lambda)\mathbf{C}_n(\lambda) = E_n(\lambda)\mathbf{C}_n(\lambda) \tag{4}$$

with the normalization condition

$$\mathbf{C}_n^\dagger(\lambda)\mathbf{C}_n(\lambda) = 1 \tag{5}$$

where $\mathbf{H}(\lambda) = \mathbf{\Phi}^\dagger H(\lambda)\mathbf{\Phi}$. Solving eqs 4 and 5 usually entails the determination of the energies $E_n(\lambda)$ and wave functions $\psi_n(\lambda)$. This may be readily accomplished through well-developed diagonalization techniques for solving both full and large sparse matrices.[24,25] However, the goal in this work is not to find the energies but, rather, to elucidate the potential from a set of energies to be measured through spectroscopic techniques. The determination of the Hamiltonian parameters (e.g., the expansion coefficients of the potential in a suitable basis) in eqs 4 and 5 requires the solution of nonlinear equations.

Beginning with eqs 4 and 5, we derived a system of PEMs for evolving a family of Schrödinger equations characterized by parameters λ in the Hamiltonian.[16−18] The procedure calls for only a single traditional solution of the Schrödinger equation at a reference parameter value λ_0, and then the PEMs are solved as functions of λ for the additional desired solutions. Both $E_n(\lambda)$ and $\mathbf{C}_n(\lambda)$ may be determined with PEMs as functions of the Hamiltonian parameter λ, which might represent nuclear charge or internuclear distance. Simultaneous multiparameter evolution may also be treated. The quantum single-state parametric equations of motion (ss-PEM) derived in ref 18 are

$$\frac{\mathrm{d}E_n}{\mathrm{d}\lambda} = \mathbf{C}_n^\dagger(\lambda)\mathbf{H}'\mathbf{C}_n(\lambda) \tag{6}$$

and

$$\frac{\mathrm{d}\mathbf{C}_n}{\mathrm{d}\lambda} = (\mathbf{H}(\lambda) - \mathbf{E}_n(\lambda) + \mathbf{N}(\lambda))^{-1}((\mathbf{C}_n^\dagger(\lambda)\mathbf{H}'\mathbf{C}_n(\lambda)) - \mathbf{H}')\mathbf{C}_n(\lambda) \tag{7}$$

where the projection matrix $\mathbf{N}(\lambda)$, which makes the matrix $(\mathbf{H}(\lambda) - \mathbf{E}_n(\lambda) + \mathbf{N}(\lambda))$ invertible, is defined by

$$\mathbf{N}(\lambda) = \mathbf{C}_n(\lambda)\mathbf{C}_n^\dagger(\lambda) \tag{8}$$

$\mathbf{E}_n(\lambda)$ is the eigenvalue $E_n(\lambda)$ multiplied by the identity matrix $\mathbf{I}$, and $\mathbf{H}'$ represents $\mathrm{d}\mathbf{H}/\mathrm{d}\lambda$. Equation 6 is a matrix formulation of the Hellmann−Feynman theorem.[16,26,27] In practice, $(\mathbf{H}(\lambda) - \mathbf{E}_n(\lambda) + \mathbf{N}(\lambda))$ is not explicitly inverted in eq 7, but rather, an LU decomposition of the matrix is performed to determine the derivative of $\mathbf{C}_n(\lambda)$. The ss-PEM method can evolve the nth energy level $E_n(\lambda)$ and its wave function $\mathbf{C}_n(\lambda)$ from an initial solution at λ_0 without knowledge of the other energy levels or wave functions. Additional energies and wave functions can be easily calculated by propagating more ss-PEM equations.

The PEM method may be easily modified for the inverse problem. If M energies $E_n(\lambda_2)$ are known at $\lambda = \lambda_2$ but M parameters $v_j(\lambda_2)$ ($j = 1, ..., M$) within the Hamiltonian are unknown at $\lambda = \lambda_2$, the ss-PEM technique can be utilized to find the M unknown parameters $v_j(\lambda_2)$. In practice, the number of input energies and potential parameters need not be the same. The only information, required by the PEM equations, is the known set of $E_n(\lambda_2)$ at $\lambda = \lambda_2$ and an initial guess for the Hamiltonian parameters at $\lambda = \lambda_2$, which we define to be the values of the Hamiltonian parameters $v_j(\lambda_1)$ at $\lambda = \lambda_1$. Once the parameters $v_j(\lambda_1)$ are initialized, the values of $E_n(\lambda_1)$ and $\mathbf{C}_n(\lambda_1)$ may be calculated at the beginning of the trajectory $\lambda = \lambda_1$ through diagonalization. Here λ plays the role of an evolutionary independent variable characterizing the inverse process of moving from the reference potential specified by $v_j(\lambda_1)$ to its final inverted form of $v_j(\lambda_2)$. As in the forward PEM solution of $E_n(\lambda)$ and $\mathbf{C}_n(\lambda)$ as functions of λ, eq 7 may be used to propagate $\mathbf{C}_n(\lambda)$. Now, however, we want to use eq 6 to propagate $v_j(\lambda)$ rather than $E_n(\lambda)$. The Hellmann−Feynman theorem in eq 6 may be rewritten to express the linear relationship between the energy changes and the changes in the Hamiltonian parameters

$$\frac{\mathrm{d}\mathbf{E}(\lambda)}{\mathrm{d}\lambda} = \mathbf{T}\frac{\mathrm{d}\mathbf{v}(\lambda)}{\mathrm{d}\lambda} \tag{9}$$

The column vectors $\mathrm{d}\mathbf{E}(\lambda)/\mathrm{d}\lambda$ and $\mathrm{d}\mathbf{v}(\lambda)/\mathrm{d}\lambda$ contain the changes in the M energy levels E_n and the M Hamiltonian parameters v_j, respectively, and $\mathbf{T}$ is a transformation matrix which interconverts these changes. We define $\mathbf{T}$ to make eqs 6 and 9 equivalent. The most important feature of the Hellmann−Feynman theorem in the i-PEM is that it provides a linear relationship between the energy and the potential changes. Within eq 4 the relationship between the energies and the potential parameters is highly nonlinear because the Hamiltonian, the wave functions, and the energies depend on the potential in a complicated manner. While most papers on chemical inversion utilize the Hellmann−Feynman theorem in the guise of first-order perturbation theory,[11−15,28,29] the i-PEM method will employ higher-order derivatives of the relation to propagate the energy levels as well as the potential efficiently along a trajectory toward the target energies and a realistic potential.

To apply the i-PEM technique, we must choose a trajectory for the energy levels as a function of the perturbation parameter λ to guide the evolution of $v_j(\lambda)$. We have the freedom of choosing the trajectory because there is no unique path between $v_j(\lambda_1)$ and $v_j(\lambda_2)$. Since we know the values of $E_n(\lambda)$ at both $\lambda = \lambda_1$ and $\lambda = \lambda_2$, we want to choose the first derivatives of the energies with respect to λ in the interval $[\lambda_1,\lambda_2]$ to ensure that the correct energies at $\lambda = \lambda_2$ are achieved. The natural

assumption is to choose the first derivatives for the M energies within the interval $[\lambda_1,\lambda_2]$ to be constant

$$\frac{dE_n(\lambda)}{d\lambda} = \frac{E_n(\lambda_2) - E_n(\lambda_1)}{\lambda_2 - \lambda_1} \tag{10}$$

While this choice accounts sensibly for where the energies should be at λ_2, it fails to consider the complicated landscape of the potential as it deforms as a function of λ. The potential will not always be able to move smoothly with these linear changes in the energies. This constitutes a representability problem. Not every smooth trajectory for the M energies may be represented by a smooth trajectory in the M potential parameters. To treat this problem, we require a flexible strategy for choosing the energy changes which efficiently balance the two goals: (1) reaching the known energy levels at λ_2 and (2) keeping the potential trajectory smooth. The key to understanding when an energy change may be represented by a smooth potential change lies in the invertibility of the transformation matrix **T**. For the inverse problem, **T** must be inverted to generate the changes in the Hamiltonian parameters $d\mathbf{v}(\lambda)/d\lambda$ from the known shifts in the energy levels. When the **T** matrix is well-conditioned, its inverse may be easily calculated to solve the linear algebraic eq 9. However, if some of the eigenvalues of the **T** matrix are much smaller than the largest eigenvalue, the **T** matrix will be nearly singular or ill-conditioned, and the resulting potential will become unsmooth from the large changes in the potential parameters.

A remedy for this undesirable behavior of the potential trajectory may be found from the singular value decomposition (SVD)[1,30] of **T**

$$\mathbf{T} = \mathbf{P}\boldsymbol{\Sigma}\mathbf{Q}^T \tag{11}$$

where **P** and **Q** are orthonormal matrixes whose columns contain the eigenvectors of $\mathbf{T}\mathbf{T}^T$ and $\mathbf{T}^T\mathbf{T}$, respectively. Both $\mathbf{T}\mathbf{T}^T$ and $\mathbf{T}^T\mathbf{T}$ possess the same set of nonnegative eigenvalues, $\{\sigma_n^2\}$. The diagonal matrix $\boldsymbol{\Sigma}$ contains the square roots of these eigenvalues, $\{\sigma_n\}$. The singular value decomposition exists for any $(m \times n)$ matrix, although we are specifically interested in the transformation matrix **T** which is square $(M \times M)$ and nonsymmetric. The SVD is a standard procedure for inverse problems[1,2] and is employed frequently in chemical inversion.[11−15] However, in the i-PEM, we use the SVD for smoothing the potential trajectory through λ space rather than simply smoothing the potential surface. The need for smoothing the trajectory only arises because i-PEM are a path-following procedure. From the singular value decomposition, it follows that

$$\mathbf{T}\mathbf{q}_n = \sigma_n\mathbf{p}_n \tag{12}$$

where $\mathbf{q}_n$ and $\mathbf{p}_n$ denote the nth columns of the matrixes **Q** and **P**. The M orthonormal vectors $\mathbf{p}_n$ span the column space of the Hamiltonian matrix **H**. Because of this, we can expand the energy changes in terms of these vectors

$$\frac{d\mathbf{E}(\lambda)}{d\lambda} = \sum_{n=1}^{M} a_n(\lambda)\mathbf{p}_n(\lambda) \tag{13}$$

The magnitude of the expansion coefficients $a_n(\lambda)$ will reflect the magnitude of the energy changes which will not be too large for a smooth trajectory. Multiplying eq 13 by $\mathbf{T}^{-1}$ and employing eqs 11 and 12, we can write the change in the Hamiltonian parameters as

$$\frac{d\mathbf{v}(\lambda)}{d\lambda} = \sum_{n=1}^{M} r_n(\lambda)\mathbf{q}_n(\lambda) \tag{14}$$

where $r_n(\lambda)$ is

$$r_n(\lambda) = \frac{a_n(\lambda)}{\sigma_n(\lambda)} \tag{15}$$

Hence, the largest ratios $r_n(\lambda)$ will determine the magnitude of the potential changes. To achieve a rapid evolution in λ, we want both the energy and potential trajectories to be as smooth as possible. However, small-energy expansion coefficients do not guarantee that the potential expansion coefficients will have similar magnitudes because one or more eigenvalues $\sigma_n(\lambda)$ may be small if the **T** is singular.

Within the i-PEM, we implement the following procedure for dealing with transformation matrixes **T** with small eigenvalues:

1. At each step of the i-PEM through λ, we choose energy derivatives which would take us linearly from the current position in λ to the target energies at λ_2. These derivatives are defined in eq 10, where λ_1 represents here the current value rather than the initial value of λ.
2. The SVD of **T** is performed as in eq 11.
3. The energy expansion coefficients are calculated from eq 13, in which we know the energy derivatives and **p** from the first two steps.
4. With eq 15, we solve for the expansion coefficients $r_n(\lambda)$ of the potential change.
5. If the coefficients $r_n(\lambda)$ are larger than a chosen threshold value ϵ, they are not included in the calculation of the potential change in eq 14. By eq 15, this is equivalent to setting the $a_n(\lambda)$, which corresponds to large $r_n(\lambda)$, to zero.
6. Using the final potential change, we find the corresponding changes in $E_n(\lambda)$ and $C_n(\lambda)$ with eqs 9 and 7, respectively.

An important property of the SVD is that neglecting the large $r_n(\lambda)$ values gives us energy changes which are as close as possible in a least-squares sense to the linear energy changes while keeping the potential trajectory smooth according to a threshold criterion ϵ. Thus, the SVD helps to determine energy changes which may be represented by locally realistic potential changes.

B. Spectral Expansion of the Potential and Wave Function. In addition to the PEM stepping and the SVD strategy, there are two other significant features of the present i-PEM method: (1) the use of spectral elements to solve the vibrational Schrödinger equation initially and to represent its PEM evolution and (2) the expansion of the potential region to be modified with Legendre polynomials. The spectral element method, originally proposed by Patera,[20] depends on the partitioning of the coordinate space into p regions (or elements), within each of which the underlying solution of the differential equation is represented by a spectral expansion.[21,22] The wave function in each element is separately expanded in a basis set of Lagrangian interpolants. While we will discuss spectral elements in the context of the one-dimensional case, the technique is readily extended to multiple dimensions through tensor products of the Lagrangian interpolants in each dimension. The portion of the wave function in the jth element will have the expansion

$$\psi_n^j(x) = \sum_{i=0}^{N} \psi_n^j(x_i)L_i(x) \tag{16}$$

where the Lagrangian interpolants are

$$L_i(x) = \frac{\prod_{k\neq i}(x - x_k)}{\prod_{k\neq i}(x_i - x_k)} \tag{17}$$

and x_i are the roots of the derivative of the Nth Legendre polynomial plus the endpoints of the interval. These points x_i are usually called Gauss−Lobatto Legendre (GLL) nodes. The ith Lagrangian interpolant for the points $\{x_i\}$ equals 1 at the ith grid point x_i and vanishes identically at the other grid points. The necessary integrals are performed with the Gauss−Lobatto Legendre quadrature, which uses the same set of points $\{x_i\}$. As is well-known from the literature on the discrete variable representation (DVR),[31] the potential energy function translates into a diagonal matrix in a basis of Lagrangian interpolants. Whether the global domain is divided into elements or not, the potential is diagonal. The advantage of domain decomposition with Lagrangian interpolants is that the derivatives in the kinetic energy operator only couple interpolants within the same element. This increases the sparsity of the resulting Hamiltonian matrix. Unlike standard finite element methods, the spectral elements employ high-order expansions on each element to maintain the exponential convergence of traditional spectral methods. The elements are weakly coupled by the continuity of the wave function. Lagrangian basis functions on the boundary of two elements will have contributions to the kinetic energy part of the Hamiltonian from both of these elements. Because the spectral element method employs the variational formulation of the Schrödinger equation

$$E_n = \int \frac{\hbar}{2m}\nabla\psi_n^*\nabla\psi_n + \psi_n V(x)\psi_n \, dx \tag{18}$$

the first derivatives do not need to be explicitly matched at the interfaces. The continuity of the first derivatives will automatically be satisfied with an accuracy corresponding to the convergence of the basis expansion.

By representing the Hamiltonian and with a different basis expansion in each region, we can use spectroscopic energy data in the spectral element method to modify only selected parts of a model potential. Often, spectroscopic data are only relevant to identifying certain features of the potential energy surface. Permitting the whole surface to change would simply render **T** even more ill-conditioned. On an element where we wish to evolve the potential, we may write the potential in terms of that element's Lagrangian interpolants

$$V(x,\lambda) = \sum_{i=0}^{N} V(x_i,\lambda)L_i(x) \tag{19}$$

We transform the potential $V(x,\lambda)$ from the Lagrange basis to a basis of Legendre polynomials $P_j(x)$

$$V(x,\lambda) = \sum_{j=0}^{N} \upsilon_j(\lambda)P_j(x) \tag{20}$$

The expressions for the potential in eqs 19 and 20 are equivalent. Because we utilize the Gauss−Lobatto Legendre points for the interpolation, both potential expressions converge exponentially fast as N increases. The spectral elements generate an accurate local approximation for the wave function and potential. The number of points in the spectral element $N + 1$ will usually be much larger than the number of known energy levels M. This is necessary to provide an accurate representation of the underlying vibrational Schrödinger equation. Hence, there are more unknown potential expansion coefficients $\upsilon_j(\lambda)$ than energy levels M. We could still solve for the potential by supplementing explicitly the energy equations with smoothness conditions in the SVD, but we explore a different approach here. The Legendre expansion for the potential in eq 20 may be truncated to its first M terms

$$\tilde{V}(x,\lambda) = \sum_{j=0}^{M-1} \upsilon_j(\lambda)P_j(x) \tag{21}$$

As described earlier, we then use this expression (eq 21) with the Hellmann−Feynman theorem in eq 9 to solve for the changes in the M potential parameters from the changes in the M known energies. Since the Legendre expansion converges exponentially for smooth functions, the truncation error will be approximately equal to the first neglected term $|\upsilon_M(\lambda)|$ in eq 21.[32] In more than one dimension, we would employ the tensor products of Legendre polynomials in each coordinate. If $V(\lambda_1)$ and $V(\lambda_2)$ are not too different from each other, the truncation error introduced into the initial potential $V(x,\lambda_1)$ will provide a method for estimating the number M of known energy levels $E_n(\lambda_2)$ required to obtain an accurate representation of the potential at $\lambda = \lambda_2$. We may utilize the truncated potential $\tilde{V}(x,\lambda_1)$ to calculate the initial energies and wave functions at $\lambda = \lambda_1$. Propagation of the potential parameters $\upsilon_j(\lambda)$ through the λ parameter space may then be accomplished using the i-PEM method with the SVD stepping strategy. At $\lambda = \lambda_2$, the first M energies equal the known energies, and the potential corresponds to an approximation of the desired potential. Because the underlying inverse spectral problem is ill-posed, different potentials could produce the same set of M eigenvalues. In the i-PEM algorithm, the problem is "regularized" by (i) starting with a spatially smooth potential at $\lambda = \lambda_1$ and (ii) using the SVD to select only smooth changes in $\upsilon_j(\lambda)$ for the evolution to $\upsilon_j(\lambda_2)$.

III. Applications

To illustrate the i-PEM method, we consider the Morse potential as a model for hydrogen fluoride. Although diatomic molecules such as HF can be treated effectively through other techniques such as RKR,[10] they furnish a convenient testing ground at this point for i-PEM. The Schrödinger equation for HF may be written as

$$-\frac{\hbar}{2\mu}\frac{d^2\psi_n(\lambda)}{dx^2} + V(x,\lambda)\psi_n(\lambda) = E_n(\lambda)\psi_n(\lambda) \tag{22}$$

in which $x = r - r_0$ represents the displacement from the equilibrium internuclear separation r_0 and $\mu = {}^{19}/_{20}$ is the reduced mass. At $\lambda = \lambda_1$, we choose an initial non-Morse approximation $V(x,\lambda_1)$ to the Morse potential $V_{\text{exact}}(x)$, which will be viewed as the exact potential. Using the i-PEM technique, we then evolve this initial guess $V(x,\lambda_1)$ through the λ -parameter space to a more accurate approximation $V(x,\lambda_2)$, which reproduces a supplied set of Morse energies. The Morse potential has the form

$$V_{\text{exact}}(x) = D(e^{-2ax} - 2e^{-ax}) \tag{23}$$

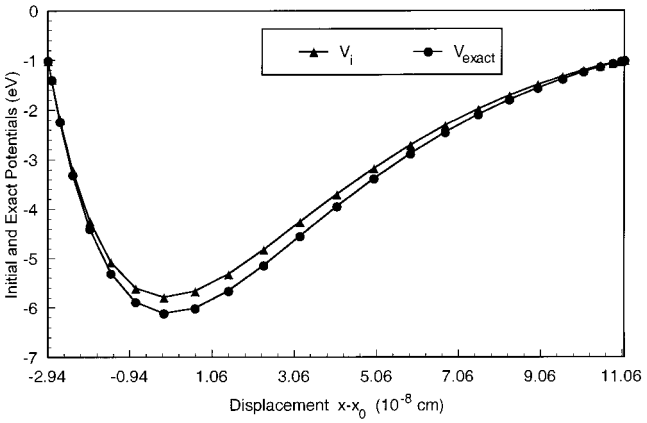

Figure 1. Initial model potential and the exact Morse potential displayed in the region where they differ. Applying i-PEM with the first 14 energy levels (ranging from -5.8598 to -1.1484 eV) yields a potential which agrees with the exact Morse potential to about 8 decimals at the interpolation points.

where in the case of HF

$$a = w\sqrt{\frac{\pi c\mu}{\hbar D}}$$

$$D = 49310 \text{ cm}^{-1}$$

$$w = 4139 \text{ cm}^{-1}.$$

The energies E_n^{exact} of the Morse model may be calculated to high accuracy by the formula

$$E_n^{\text{exact}} = -D + (n + {}^1/_2)w - \frac{(n + {}^1/_2)^2 w^2}{4D} \qquad (24)$$

Like spectroscopic data, these energies E_n^{exact} correspond to the energies from a complete basis. In practice, we must use a finite basis set whose matrix Hamiltonian in the projected space may have an eigenvalue spectrum that deviates from the exact energy spectrum E_n^{exact}. By choosing a large basis set, however, we can minimize these deviations.

To represent the wave functions, we partition the coordinate space into three spectral elements, on each of which the wave function is expanded in terms of Lagrangian interpolants at Gauss−Lobatto Legendre (GLL) nodes. Mappings are performed to match the three regions of coordinate space with the domain $[-1,1]$ of the Legendre polynomials $P_n(u)$. The elements I and III which cover the asymptotic regions of the potential curve employ an algebraic mapping that stretches the domain $[-1,1]$ to $(-\infty,a]$ and $[b,\infty)$, respectively. The mapping for element I has the form

$$x = L_{\text{I}}\left(\frac{u-1}{1.0001+u}\right) + a \qquad (25)$$

in which L_{I} (8×10^{-10}) is a stretching parameter. We employ a similar mapping for element III

$$x = L_{\text{III}}\left(\frac{1+u}{1.0001-u}\right) + b \qquad (26)$$

where L_{III} (4×10^{-9}) is also a stretching parameter while the finite domain $[a,b]$ for element II requires only a linear mapping

$$x = \frac{b-a}{2}u + \frac{b+a}{2} \qquad (27)$$

The initial potential is allowed to vary in element II while elements I and III, extending over the asymptotic regions, remain fixed. We choose element II to include the portion of the Morse potential that is less than -1 eV; with this criterion, we calculated the values for a and b, which are approximately -2.9357×10^{-9} cm and 1.1119×10^{-8} cm. The initial model potential and the exact potential for element II are shown in Figure 1. Weak coupling of the three spectral elements produces a sparse Hamiltonian matrix with three overlapping blocks on the diagonal. The overlap of the blocks imposes the essential continuity of the wave function.

In addition to the approximation of the underlying Hilbert space, which determines how well we reproduce the exact energy levels E_n^{exact}, the accuracy of the final potential also depends on the flexibility of the potential model. To maximize flexibility and accuracy, we utilize an expansion in terms of Legendre polynomials

$$V(u,\lambda) = a(1-u) + b(1+u) + (1-u)(1+u)\sum_{n=0}^{N_2-3} \upsilon_n(\lambda)P_n(u) \qquad (28)$$

to represent the potential on element 2 where u, the mapped variable, is defined on $[-1,1]$, a and b are the fixed values of the potential at the boundaries of elements I and II and elements II and III, respectively, and N_2 indicates the number of Lagrange functions inside element II. Using spectral elements is important because a Legendre expansion of the whole potential would not converge spectrally, since the potential becomes infinite as $|x|$ approaches infinity. Furthermore, the GLL nodes of element II are the optimal N_2 interpolation points for generating a Legendre polynomial expansion of order $N_2 - 1$ on element II. Lagrange interpolants of one global element would not correspond to the optimal interpolation points of the local Legendre expansion. On element II, the sequence of expansion coefficients $\upsilon_n(\lambda)$, decreasing rapidly in magnitude, can be truncated after M terms to produce a spectrally accurate approximation to the potential at λ_2.

The Morse potential curve for HF and the initial guess are shown in Figure 1. Evolving the potential through the λ parameter space with the first 14 energy levels produces a potential which agrees with the exact Morse potential at the GLL nodes to ~8 decimals. More accuracy can be achieved by following more energy levels. The initial guess for the potential, which was too high in energy, relaxes naturally into the exact potential to satisfy the 14 known energy levels. For this calculation, we used the first 14 energy levels of the (6,24,6)-Hamiltonian matrix (the **H** matrix formed from 6 GLL cardinal functions in elements I and III and 24 GLL cardinal functions in element II) rather than the exact Morse energies. In a finite basis set with the eigenvalues of the Hamiltonian matrix, the energy levels of the truncated space may deviate from the exact Morse energies in the complete Hilbert space. Figure 2 presents the average error in the first 15 energy levels for basis sets of different sizes when compared with the exact Morse energies. The rapid lengthening of the bars with increasing basis set size demonstrates the exponential convergence of the spectral elements. Employing energies from the complete space (i.e., simulated experimental values) to determine a potential in the truncated space will naturally introduce errors. The second source of error in the potential arises from the M energy levels that are followed to determine the first M terms of the Legendre expansion. By using energy levels from the truncated space as the "known" Morse energies, we may suppress the first source

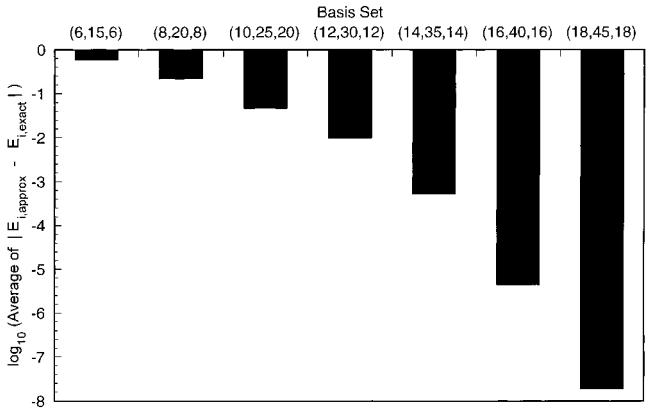

Figure 2. Average error in the first 15 energy levels (eV) given for 7 different basis sets of spectral elements. The bar graph illustrates the exponential convergence of the basis with the number of grid points.

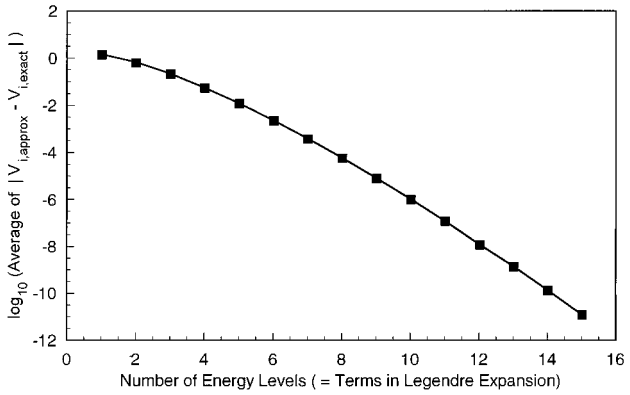

Figure 3. Potential approximation from i-PEM converging exponentially with the number M of known energy levels. Each additional energy level allows us to calculate another term in the Legendre expansion and, hence, the spectral convergence. The potential error (eV) is calculated from an average of the absolute errors at the interpolation nodes.

of error in the calculation to explore more fully the error from the truncation of the potential expansion at M terms with this procedure. Figure 3 shows that the accuracy of the Legendre potential expansion increases exponentially as additional terms are added. The fast convergence of the spectral potential expansion allows for extracting a nearly optimal amount of information about the potential from the known M energy levels.

Unlike traditional PEM where known changes in a reference potential are employed to find new energy levels, the i-PEM invert this process by using known changes in the energy levels to determine the appropriate modifications of the reference potential. The main difficulty of the inverse process arises from the fact that small changes in energy can produce large changes in the potential. In section II, we expressed this mathematically by noting that the changes in energies and potential parameters are connected by a transformation matrix **T**, as shown in eq 9. Expressing the changes in the energies and the potential parameters as in eqs 13 and 14 demonstrates how a small change in the energy can correspond to a big change in the potential when some of the eigenvalues σ_i are small compared to the size of the expansion coefficients a_i. This difference in magnitude is shown in Figure 4, where the values of a_i and r_i are given for different values of i at the beginning of the i-PEM evolution of 14 energy levels of the (6,24,6)-Hamiltonian. We see that the magnitude of the potential expansion coefficient r_{14} is much larger than any of the energy expansion coefficients a_i's. Because the changes in the potential parameters will be so

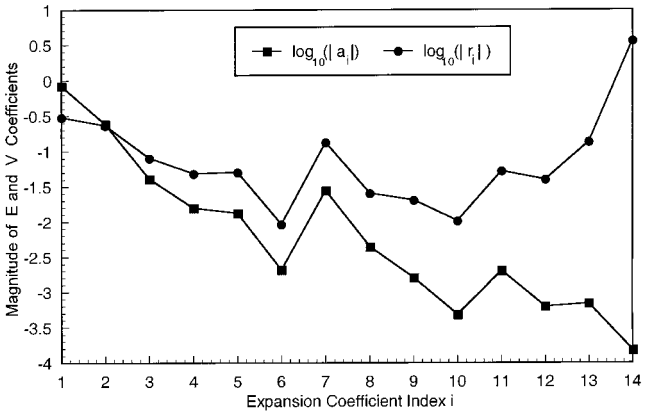

Figure 4. Two expansion coefficients a_i and r_i for the energy and potential changes displayed in a logarithmic plot of their absolute values for the first i-PEM step. Because the magnitude of r_{14} is greater than 1, we eliminate it from the potential's Taylor series expansion in λ to increase convergence.

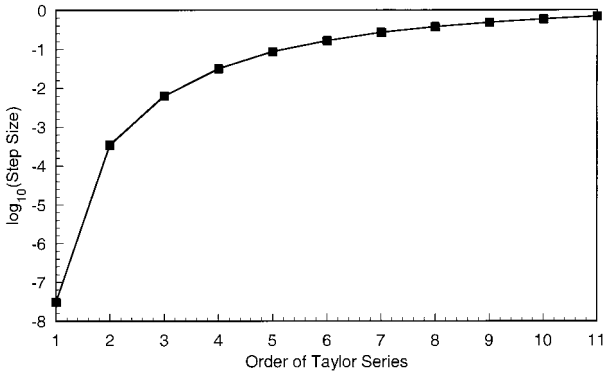

Figure 5. Logarithm of the step size given as a function of the Taylor series order in λ. The i-PEM's ability to invoke high orders enables large steps through the λ parameter space.

much larger than the corresponding changes in the energies, only small steps in λ will be permitted.

The i-PEM/SVD procedure, introduced in section II A, surmounts this problem by following a path for the change in energies that balances the smoothness in the potential and energy trajectories. The optimal path will be one which allows us to move as close to the final energies as possible after each step. If we set $a_{14} = 0$ in eqs 13 and 14, as prescribed in step 5 of the i-PEM algorithm, then r_{14} also vanishes, and we significantly decrease the magnitude of the potential change. The λ-Taylor series for the potential now will not diverge. For the first step in the HF calculation, Figure 5 presents the step size in λ as a function of the Taylor Series order. By invoking high orders, the i-PEM method takes a large step in the direction of the target energies. The target energies are achieved when the step size equals unity and all of the singular values are included. As the norm of $d\mathbf{E}/d\lambda$ decreases with the steps of i-PEM, the magnitudes of the energy expansion coefficients a_i also diminish. If the magnitude of the singular value $1/\sigma_{14}$ remains relatively constant, the magnitude of the potential expansion coefficient r_{14} (a_{14}/σ_{14}) will also decrease. In Table 1, the absolute values of a_{14}, σ_{14}, and r_i are reported as functions of the number of steps. Because the magnitude of r_{14} decreases significantly after the first step, the r_{14} coefficient may then be included in the potential expansion without disrupting the potential's trajectory through the λ parameter space. Energy errors in Table 1 are measured by reporting the largest deviation observed in the 14 energy levels. After only six λ steps, the i-PEM method reaches

TABLE 1: Step Size, Taylor Series Order, Energy Error, and the Magnitudes of the Expansion Coefficients for the Energies and the Potentials of the Six i-PEM Steps of the HF Calculation

step number	step size	order	energy error	$\lvert a_{14}\rvert$	$\lvert \sigma_{14}\rvert$	$\lvert r_{14}\rvert$
1	0.693	11	-9.97×10^{-2}	1.51×10^{-4}	4.11×10^{-5}	3.67
2	0.234	9	-7.64×10^{-2}	1.34×10^{-5}	1.67×10^{-5}	8.02×10^{-1}
3	0.345	10	-5.01×10^{-2}	5.67×10^{-6}	1.49×10^{-4}	3.80×10^{-1}
4	0.408	9	-2.96×10^{-2}	4.35×10^{-9}	1.35×10^{-5}	3.21×10^{-4}
5	0.263	6	-2.18×10^{-2}	1.81×10^{-6}	1.29×10^{-5}	0.140
6	1.000	9	0	1.86×10^{-6}	1.28×10^{-5}	0.145

the exact target energies and generates a potential which is correct to 8 decimals.

IV. Conclusions

A new approach for using spectroscopic rovibrational data to generate realistic potential surfaces has been presented. The method, known as the inverse parametric equations of motion (i-PEM), evolves from an initial model potential to an improved potential as a function of the rovibrational energy levels. We address the problem of finding an efficient energy path that leads to the target spectroscopic energies. There is an underlying representability problem in that not every trajectory of energy levels may be represented by a smooth trajectory in the potential. This problem appears in the ill-conditioned transformation matrix **T**, which converts changes in the potential to changes in the energies. With the singular value decomposition of **T**, a strategy was developed for moving systematically in the direction of the target energies while keeping the trajectory of the potential smooth.

Spectroscopic energy data are often relevant to refining features in specific parts of the potential surface. However, DVR expansions that cover the global domain in a single expansion are often employed to represent large potential energy surfaces.[33,34] We propose the use of spectral elements[20−23] for solving the rovibrational Schrödinger equation. As a domain decomposition method, the spectral elements represent the wavefunction with separate Lagrange basis expansions on each element. Because it uses the variational formulation of the Schrödinger equation, the technique only requires imposing continuity of the wave function across elemental boundaries. With spectral elements, the potential matrix is diagonal, as with DVR, but the kinetic energy matrix is also sparse because the derivatives only couple interpolants on the same element. While the sparsity of the Hamiltonian is increased, spectral element methods use sufficiently large expansions on each domain to preserve the exponential convergence of the wave function with the number of grid points that is characteristic of DVR and other global spectral methods.[21,22] Domain decomposition methods provide a natural approach to focusing attention on a specific region of the potential for improvement. We show that the spectral elements may be combined with a Legendre expansion on the elements selected for alteration.

Application of the i-PEM method was made to a simulated inversion of the vibrational energy levels of hydrogen fluoride. Using 14 energies, we evolved an initial approximation or the HF potential to a final potential that was equivalent to the Morse potential to within 10^{-8} eV. Additional accuracy may be achieved by including more energy levels. The example illustrates how the local Legendre expansion helps through its spectral convergence in obtaining a maximum amount of information from the known energy levels. Future work should extend the method to multidimensional rovibrational systems such as van der Waals clusters and problems with significant noise. As a path-following method, the i-PEM differ significantly from other inversion techniques currently employed for spectroscopic inversion. The present work lays the foundation for combining PEM and spectral elements to produce a new tool for revealing the landscapes of potential energy surfaces.

Acknowledgment. D.A.M. thanks Dr. Paul F. Batcho for sharing with the author his enthusiasm for spectral elements. D.A.M. also thanks Professor Dudley R. Herschbach and Dr. Alexander R. Mazziotti for their encouragement and helpful discussion. The authors acknowledge the NSF and DOE for their support.

References and Notes

(1) Hansen, P. C. *Rank-Deficient and Discrete Ill-Posed Problems: Numerical Aspects of Linear Inversion*; SIAM: Philadelphia, 1998.
(2) Chu, M. T. *SIAM Rev.* **1998**, *40*, 1.
(3) Cuppen, J. J. M. Numerical Solution of the Inverse Problem of Electrocardiography. Ph.D. Thesis, University of Amsterdam, Amsterdam, The Netherlands, 1983.
(4) Thorpe, A. J.; Scharf, L. L. *IEEE Trans. Signal Process* **1995**, *43*, 1591.
(5) Levy, M. *Adv. Quantum Chem.* **1990**, *21*, 69.
(6) Coleman, A. J. *Rev. Mod. Phys.* **1963**, *35*, 668.
(7) Mazziotti, D. A. *Phys. Rev. A* **1998**, *57*, 4219.
(8) Mazziotti, D. A. *Chem. Phys. Lett.* **1998**, *289*, 419.
(9) Mazziotti, D. A. *Int. J. Quantum Chem.* **1998**, *70*, 557.
(10) Rydberg, R. *Z. Phys.* **1931**, *73*, 376; **1933**, *80*, 514. Klein, O. *Z. Phys.* **1932**, *76*, 226. Rees, A. L. G. *Proc. Phys. Soc.* **1947**, *59*, 998.
(11) Ho, T.; Rabitz, H. *J. Phys. Chem.* **1993**, *97*, 13447.
(12) Ho, T.; Rabitz, H.; Choi, S.; Lester, M. *J. Chem. Phys.* **1995**, *102*, 2282.
(13) Zhang, D. H.; Light, J. C. *J. Chem. Phys.* **1995**, *103*, 9713.
(14) Wu, Q.; Zhang, D. H. *Chem. Phys. Lett.* **1996**, *252*, 195.
(15) Wu, Q.; Zhang, D. H. *J. Chem. Phys.* **1997**, *107*, 3607.
(16) Mazziotti, D. A.; Mishra, M. K.; Rabitz, H. A. *J. Phys. Chem.* **1995**, *99*, 112.
(17) Mazziotti, D. A. An Evolutionary Approach to Determining Quantum Bound-State Energy Eigenvalues and Eigenvectors Using Parametric Equations of Motion. Senior Thesis, Princeton University, Princeton, NJ, 1995.
(18) Mazziotti, D. A.; Rabitz, H. A. *Mol. Phys.* **1996**, *89*, 171.
(19) Gupta, A. K.; Gross, P.; Bairagi, D. B.; Mishra, M. K. *Chem. Phys. Lett.* **1996**, *257*, 658.
(20) Patera, A. T. *J. Comput. Phys.* **1984**, *54*, 468.
(21) Canuto, C., et al. *Spectral Methods in Fluid Dynamics*; Springer-Verlag: New York, 1988.
(22) Boyd, J. P. *Chebyshev and Fourier Spectral Methods*; Lecture Notes in Engineering 49; Springer-Verlag: New York, 1989.
(23) Batcho, P. F. *Phys. Rev. A* **1998**, *57*, 4226.
(24) Smith, B. T., et al. *Matrix Eigensystem Routines - EISPACK Guide*, 2nd ed.; Springer-Verlag: New York, 1976.
(25) Lehoucq, R. B.; Sorensen, D. C.; Yang, C. *ARPACK User's Guide: Solution of Large-Scale Eigenvalue Problems with Implicitly Restarted Arnoldi Methods*; SIAM: Phildelphia, 1998.
(26) Feynman, R. P. *Phys. Rev.* 1939.
(27) *The Force Concept in Chemistry*; Deb, E., Ed.; Van Nostrand Reinhold: New York, 1981.
(28) Kosman, W. M.; Hinze, J. *J. Mol. Spectrosc.* **1975**, *56*, 93.
(29) Hamilton, I. P.; Light, J. C.; Whaley, K. B. *J. Chem. Phys.* **1986**, *85*, 5151.
(30) Press, W. H., et al. *Numerical Recipes in FORTRAN: The Art of Scientific Computing*, 2nd ed.; Cambridge University Press: New York, 1992.
(31) Bacic, Z.; Light, J. *J. Chem. Phys.* **1986**, *85*, 4594.
(32) Fox, L.; Parker, I. B. *Chebyshev Polynomials in Numerical Analysis*; Oxford University Press: New York, 1968.
(33) Choi, S. E.; Light, J. C. *J. Chem. Phys.* **1990**, *92*, 2129.
(34) Korambath, P. P.; Wu, X. T.; Hayes, E. F. *J. Phys. Chem.* **1996**, *100*, 6116.